Producer/Injector Ratio: The Key to Understanding Pattern Flow Performance and Optimizing Waterflood Design

C.E. Hansen, SPE, EOG Resources Inc., and **J.R. Fanchi,** SPE, Colorado School of Mines

Summary

When designing a waterflood, the important aspect of processing rate with respect to pattern selection has not been addressed adequately in the literature. It has not been possible, using the existing analytical background, to determine and compare the flow-rate performance of all the patterns for any given rock/fluid (mobility) system. While general two-phase equations exist for the five-spot and line-drive patterns, flow equations for other patterns either have not been presented (e.g., the seven-spot) or are not sufficiently general (e.g., the nine-spot) to apply to all mobility conditions. A general treatment of skin effect also has not been given.

This paper presents a new, comprehensive analytical treatment of pattern flow for isotropic, homogeneous reservoirs that applies to all patterns and mobility conditions. This is made possible by a new equation for the volumetric average reservoir pressure of regularly spaced, repeated patterns. The new formulas demonstrate how the producer/injector ratio (*P/I*) controls reservoir pressures and flow rates and (for the first time) allow the differences in the flow capacity of patterns to be quantified. The mobility characteristics that control flow rates are described fully by a newly defined total mobility ratio, M_T. The form of the new equations allows for modifications for skin effect and reservoir heterogeneity. We show how skin effect can act disproportionately with injectors and producers because of its interaction with *P/I* and M_T.

Introduction

The economics of a waterflood depend on two primary variables that engineers seek to optimize when designing a flooding scheme: (1) the processing, or throughput rate, and (2) the incremental oil recovery. Depending on the characteristics of the reservoir, one of these objectives can take a more dominant role in the determination of the optimum flooding pattern. For example, if there is significant permeability anisotropy, incremental recovery will take precedence because of its strong dependency on producer/ injector orientation. Conversely, in isotropic reservoirs, considerations of flow rate will drive pattern selection because incremental recovery in these reservoirs is largely independent of pattern type. In both types of reservoirs, an adequate recovery rate is paramount to an economically viable project.

When attempting to optimize the flow rate of waterfloods in isotropic reservoirs, however, one quickly finds that the existing literature does not provide sufficient background to accomplish this. While waterflooding has, for the most part, a well-established technical basis, the analytical development for two-phase pattern flow rates is incomplete, most notably for the seven-spot and nine-spot patterns. Also, the existing theoretical background does not identify the fundamental mechanisms controlling pattern rates. As a result, there has been an overall lack of insight into factors controlling pattern rates and the flow-capacity differences that exist between the patterns for any two-phase system. This has required that the engineer rely largely on trial and error, numerical waterflood design processes, or field-specific experience. Given that differences in flow capacity can be quite significant depending on the mobility conditions of the reservoir, a trial-and-error approach could be unpredictable and in turn have a negative effect on the economics realized from a waterflood project. Therefore, a more complete analytical understanding of pattern flow behavior is necessary to enable the more effective use of all available design tools.

This paper presents new analytical relationships describing the two-phase, steady-state flow-rate performance of repeated patterns in homogeneous, isotropic reservoir systems. These relationships represent a general, comprehensive pattern flow theory that greatly extends the range of applicability to all patterns, mobility conditions, and stages of the flood. The theoretical development is founded on a new equation for the volumetric average reservoir pressure of patterns. We show how pattern average pressures and flow rates are a function of *P/I* and M_T. Depending on M_T, substantial differences can exist in the throughput rates achievable with the different patterns. For any M_T, there is a *P/I* that provides the highest flow capacity relative to all others. The relative differences in flow capacity become more pronounced as M_T gets increasingly larger or smaller than unity. The form of the new equations also allows a general treatment of skin effect and reservoir heterogeneity. As shown, skin effect acts as an adjustment to the physical *P/I;* as such, the pattern flow rate can be influenced disproportionately by the skin effect of one type of well (i.e., injectors or producers) over the other.

As also presented, M_T can be correlated to the endpoint mobility ratio, M, and the oil relative permeability curve shape for the prewater-breakthrough period. The correlation is based on numerical results and is useful in determining the economically optimum pattern in isotropic reservoirs using the equations presented. The new equations apply equally well to augmented waterfloods, such as polymer floods.

Background

The theory of injection patterns, or networks, extends back to the 1930s, where Muskat[1] presented analytical solutions for several patterns using "ideal" flow assumptions, which include a single-phase, incompressible fluid of constant viscosity flowing at steady-state conditions in a horizontal, homogeneous, and isotropic reservoir. Deppe[2] later presented flow equations for the ideal nine-spot pattern. The single-phase assumption also has been referred to in the literature as being equivalent to the unit-mobility ratio condition for two-phase systems (that is, when the endpoint mobility ratio, M, is equal to 1). However, as shown in this paper, this is not a sufficient criterion to apply "ideal" pattern equations to real reservoir systems. The sufficient condition that must exist is that the total mobility ratio, M_T, as defined here, is equal to one. This condition can exist in systems where $M \neq 1.0$ and does not necessarily exist when $M = 1.0$. Only when $M_T = 1.0$ can the single-phase equations be used. Thus, the applicability of the single-phase equations is limited to a small subset of reservoirs.

The flow theory for nonunit total mobility systems is not nearly as well developed. Several investigators have studied nonunit mobility ratio pattern flow behavior using a variety of techniques,[2–8] with the five-spot pattern being studied most frequently. These techniques have included a potentiometric model,[3] an X-ray shadowgraph study,[4] a scaled flow-model study,[5] and a potentiometric

This paper (SPE 86574) was revised for publication from paper SPE 75140, first presented at the 2002 SPE/DOE Improved Oil Recovery Symposium, Tulsa, 13–17 April. Original manuscript received for review 8 March 2002. Revised manuscript received 10 February 2003. Paper peer approved 29 July 2003.

model with corresponding formulas[6] of the five-spot pattern. Studies for other patterns are much less abundant and include the skewed four-spot,[7] direct-line drive,[8] and nine-spot.[2] Other nine-spot studies have been limited to the investigation of recovery curves and sweep efficiencies,[9–11] not flow rates. It must be emphasized that these methods[2–8] assume an idealized displacement mechanism (i.e., there is no saturation gradient and thus no mobility gradient within the swept region). This is equivalent to the assumption of pistonlike displacement, which can be valid when $M<<1.0$, but which is a very poor assumption when $M>1.0$. In most cases, there will be a saturation gradient in the swept region that is dependent on the shape of the relative permeability curves, even at low mobility ratios. Thus, the applicability of these studies to real systems is very limited, if not invalid, and the variety of techniques used preclude a direct comparison of the flow capacities of the patterns as a function of mobility characteristics.

To the authors' knowledge, the most rigorous analytical treatment of nonunit mobility pattern flow is given by Willhite.[12] Unlike previous works that discuss equations in nonunit mobility systems[2,6,8] where only pistonlike displacement is assumed, Willhite also considers non-pistonlike displacement where there is two-phase flow behind the flood front. To accomplish this, he introduces a total mobility ratio, M_t, that is used to account for the mobility gradient within the swept region. While rigorous, Willhite presents only the equations for the five-spot and line-drive patterns, which are valid for times up to an areal sweep efficiency of 50% (in practice, these equations should be adequate to estimate rates up to breakthrough). Note also that M_t is defined only for these patterns, where $P/I=1.0$, and it is not shown how M_t would be defined for other patterns. Because only the five-spot and line-drive patterns are considered, comprehensive flow-rate comparisons between all of the patterns with respect to total mobility ratio are not possible.

Other methods of predicting waterflooding behavior in nonunit total mobility ratio, 2D systems include numerical finite-difference simulation and analytical streamtube methods.[13–18] These methods can account for the complete fractional flow behavior without full analytical treatment. The limitation of these methods is that they do not provide the insight into the parameters governing the flow process that a representative analytical equation can provide. We believe this insight into pattern flow behavior is afforded by the relationships presented in this paper.

Theoretical Development

The basis of the new pattern flow equations is a new equation for the average reservoir pressure in isotropic, homogeneous patterns. For the assumptions of incompressible fluids flowing at steady-state conditions in a horizontal, homogeneous, and isotropic reservoir within a uniformly spaced, repeated pattern, the average reservoir pressure within any element of symmetry is given by[20]

$$\overline{p}_{\text{pat}} = \frac{\int p \times \mathrm{d}V}{\int \mathrm{d}V} = \frac{(M_T)(p_{wfI}) + (P/I)(p_{wfP})}{M_T + P/I}, \quad \ldots\ldots\ldots\ldots (1)$$

where

$$M_T = \frac{\overline{\lambda}_{TI}}{\overline{\lambda}_{TP}}, \quad \ldots\ldots\ldots\ldots (2)$$

$$\overline{\lambda}_{TI} = \frac{\sum_{j=1}^{N_I} f_{(j)} \times \lambda_{T\text{eff}(j)}}{\sum_{j=1}^{N_I} f_{(j)}}, \quad \ldots\ldots\ldots\ldots (3a)$$

and

$$\overline{\lambda}_{TP} = \frac{\sum_{j=1}^{N_P} f_{(j)} \times \lambda_{T\text{eff}(j)}}{\sum_{j=1}^{N_P} f_{(j)}}. \quad \ldots\ldots\ldots\ldots (3b)$$

In Eq. 3, $\lambda_{T\text{eff}(j)}$ is the effective total mobility of the oil and water for a given well within the pattern element, defined from the wellbore radius to the average reservoir pressure contour (see further definition below), and $f_{(j)}$ is the fraction of the well's total flow rate contributed to the pattern element.

For example, consider an element of symmetry of the inverted nine-spot pattern shown in **Fig. 1.** $\overline{\lambda}_{TP}$, the average effective total mobility of production, is calculated according to Eq. 3b as

$$\overline{\lambda}_{TP} = \frac{0.25\lambda_{T\text{eff}(2)} + 0.25\lambda_{T\text{eff}(3)} + 0.25\lambda_{T\text{eff}(4)}}{0.25 + 0.25 + 0.25}, \quad \ldots\ldots\ldots\ldots (4)$$

while $\overline{\lambda}_{TI}$, the average effective total mobility of injection, is simply equal to $\lambda_{T\text{eff}(1)}$ as the only injection well.

Determining Effective Total Mobilities. The effective total mobility for a given well, $\lambda_{T\text{eff}(1)}$, is the single mobility value, k_r/μ, that represents the pressure-drop equivalent mobility between the wellbore and the average reservoir pressure contour. For any pattern well, this definition satisfies the relationship given by

$$[\overline{p}_{\text{pat}} - p_{wf(j)}]\lambda_{T\text{eff}(1)} = p_{D(j)} q_{(j)} \frac{141.2}{kh}, \quad \ldots\ldots\ldots\ldots (5)$$

where $p_{D(j)}$ is the steady-state dimensionless pressure for a given well that accounts for the flow geometry between $p_{wf(j)}$ and $\overline{p}_{\text{pat}}$. $\lambda_{T\text{eff}(1)}$ can be estimated with the same approach outlined by Willhite for calculating an "average apparent viscosity", $\overline{\lambda}_{rf}^{-1}$, for a well[12]:

$$\overline{\lambda}_{rf}^{-1} = \frac{\int_{r_w}^{r_f} \lambda_r^{-1} \mathrm{d}r/r}{\ln(r_f/r_w)}. \quad \ldots\ldots\ldots\ldots (6)$$

This formula results from radial series averaging of total mobility between the well and some radial distance r_f. Radial flow around the wells is a good assumption for repeated patterns.[2,21] In this paper, the effective total mobility is similarly defined as

$$\lambda_{T\text{eff}} = \frac{\ln(r_{p\text{avg}}/r_w)}{\int_{r_w}^{r_{p\text{avg}}} \frac{\mathrm{d}r/r}{\overline{\lambda}_{T(r)}}}, \quad \ldots\ldots\ldots\ldots (7a)$$

where $\lambda_{T\text{eff}}$ is defined between the wellbore and the radial distance to average reservoir pressure contour, $r_{p\text{avg}}$, and $\overline{\lambda}_{T(r)}$ is the average total mobility at radius r, or

$$\overline{\lambda}_{T(r)} = \frac{1}{r\theta} \int_0^{\theta} \lambda_T \times r \times \mathrm{d}\theta. \quad \ldots\ldots\ldots\ldots (7b)$$

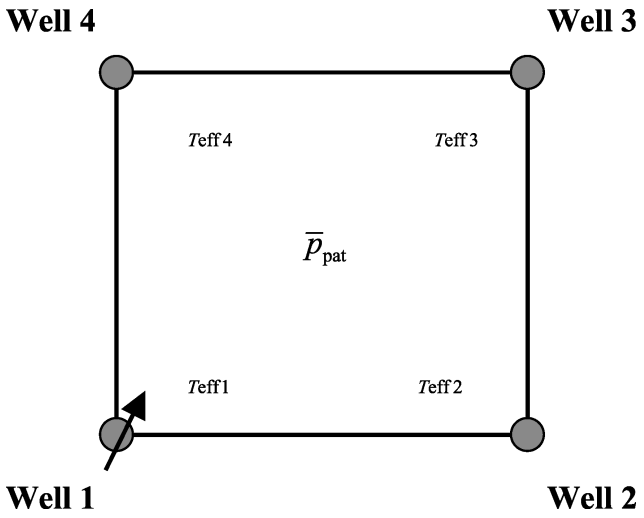

Fig. 1—Inverted nine-spot quarter element of symmetry.

In calculating $\lambda_{T\text{eff}}$ for a given well, it may seem problematic that for any pattern, the steady-state flow regime becomes increasingly nonradial away from the wells and that the location of the average pressure contour is not known *a priori* before the calculation of Eq. 1 is made. However, a study of Eq. 7 will reveal that the total mobilities closer to the well have the greatest impact on the calculation of $\lambda_{T\text{eff}}$, which is a well-known characteristic of radial flow. As a result, the mobilities farther away from a well have an increasingly smaller impact on the calculation of $\lambda_{T\text{eff}}$. Also for this reason, the flow regime away from the well, be it subradial to elliptical to linear, can be assumed radial. Thus, $\lambda_{T\text{eff}}$ can be closely approximated by using Eq. 7 out to a sufficiently large radial distance. Hansen[20] uses a numerical method to carry out the integration to a radial distance of $0.5d$ to estimate $\lambda_{T\text{eff}}$ and shows that the analytical and numerical results agree closely. Therefore, knowing the exact location of the average reservoir pressure contour or accounting for the shift away from a radial flow regime is not required to determine an accurate $\lambda_{T\text{eff}}$ for each well.

With the definitions of $\bar{\lambda}_{Tl}$, $\bar{\lambda}_{TP}$, and $\lambda_{T\text{eff}}$ given by Eqs. 3 and 5, and as approximated by Eq. 7, it can be seen that M_T represents the total mobility at every point in the reservoir and is defined for all patterns at any stage of the flood. Thus, the mobility characteristics of the reservoir as these relate to flow rate are described fully by M_T. Also, while the value of M_T changes continuously throughout the life of a flood because of changing saturations in the reservoir, its definition does not change. M_T is similar to the definition of total mobility ratio M_t given by Willhite[12]; however, his definition applies only to the five-spot and line-drive patterns up to an areal sweep of 50%.

Applicability of the Average Pressure Equation. Eq. 1 is applicable to uniformly spaced, repeated patterns. The precise meaning of "uniformly spaced" is any pattern where an element of symmetry can be drawn in which the geometric relationship between the element area and all of the element wells is the same. This definition thus includes any square or rectangular patterns such as the five-spot, direct and staggered-line drives, the nine-spot, and the hexagonal seven-spot pattern. This strict definition excludes the skewed four-spot; however, in practicality, Eq. 1 would closely approximate the average reservoir pressure for this pattern. Refs. 12 and 19 show the geometry of the various patterns. Eq. 1 is also derived assuming incompressible fluids; however, application to compressible fluids can be made with small errors (<2%) for typical oil and water compressibilities.[20]

Generalized Flow Equation for Two-Phase Patterns

The development of a general pattern flow equation will now be outlined. Additional details can be found in Ref. 20. The average reservoir pressure equation (Eq. 1) can be rewritten for the single-phase case, where $M_T = 1.0$, as

$$\frac{p_{wfl} - \bar{p}_{\text{pat}}}{\bar{p}_{\text{pat}} - p_{wfP}} = P/I. \quad \ldots\ldots (8)$$

We also know that for steady-state flow (i.e., a succession of steady states for two-phase flow),

$$P/I = \frac{\bar{q}_{\text{inj}}}{\bar{q}_{\text{prod}}}. \quad \ldots\ldots (9)$$

Combining Eqs. 8 and 9, we can write

$$\frac{p_{wfl} - \bar{p}_{\text{pat}}}{\bar{p}_{\text{pat}} - p_{wfP}} = \frac{\bar{q}_{\text{inj}}}{\bar{q}_{\text{prod}}}. \quad \ldots\ldots (10)$$

If we write general pattern flow equations for injectors and producers relative to the average reservoir pressure,

$$p_{wfl} - \bar{p}_{\text{pat}} = \frac{141.2\mu}{kh} p_{D(\text{inj})} \bar{q}_{\text{inj}} \quad \ldots\ldots (11a)$$

and

$$\bar{p}_{\text{pat}} - p_{wfP} = \frac{141.2\mu}{kh} p_{D(\text{prod})} \bar{q}_{\text{prod}}, \quad \ldots\ldots (11b)$$

we can see that the term $\frac{141.2\mu}{kh} p_D$ must be the same for both injectors and producers in Eqs. 11a and 11b to satisfy Eq. 10 [i.e., $p_{D(\text{inj})} = p_{D(\text{prod})}$]. Note that this is true only when the pressure drop is defined relative to the average reservoir pressure, which is a significant result derived from Eq. 1. Therefore, dimensionless pressure for any pattern is defined in this paper according to Eq. 11 as $p_{D(\text{pat})}$, where $p_{D(\text{pat})} = p_{D(\text{inj})} = p_{D(\text{prod})}$. Furthermore, we can solve for $p_{D(\text{pat})}$ for any pattern if we equate the single-phase equations with the generalized form of Eq. 11. For example, equating Muskat's single-phase five-spot equation[1] with Eq. 11a, we have

$$\bar{q}_{\text{inj}} = \frac{0.003541kh(\Delta P)}{\mu\left(\ln\frac{d}{r_w} - 0.619\right)} = \frac{kh(\Delta P)}{141.2 p_{D(\text{pat})}\mu} \times \frac{P/I}{1 + P/I}, \quad \ldots\ldots (12)$$

where a rearranged form of Eq. 1 has also been substituted for $p_{wfl} - \bar{p}_{\text{pat}}$ in Eq. 11a:

$$p_{wfl} - \bar{p}_{\text{pat}} = \frac{P/I}{1 + P/I}\Delta P. \quad \ldots\ldots (13)$$

The $p_{D(\text{pat})}$ for each pattern determined in this way is shown in Eqs. 14 through 17. The determination of $p_{D(\text{pat})}$ for the nine-spot is somewhat more complicated, as discussed in Appendix A. Unlike the original equations for the nine-spot,[2] the generalized single-phase flow relationship (Eq. 11) using the dimensionless pressure given by Eq. 17 is now insensitive to the value of R, the ratio of corner-to-side well flow rates, where $p_{D(\text{pat})}$ varies <1% when R<10. This is because in the equations presented by Deppe,[2] R indirectly accounts for the side and corner sandface pressures. These pressures are accounted for with the average pressure relationship, and the dependency between $p_{D(\text{pat})}$ and R now involves only effects of flow geometry. Thus, using $R = 1.0$ in Eq. 17 should be adequate for most situations when calculating $p_{D(\text{pat})}$ for the nine-spot.

Five-Spot:

$$p_{D(\text{pat})} = \ln\frac{d}{r_w} - 0.619. \quad \ldots\ldots (14)$$

Direct Line-Drive and Staggered Line-Drive:

$$p_{D(\text{pat})} = \ln\frac{a}{r_w} + 1.571\frac{d}{a} - 1.838. \quad \ldots\ldots (15)$$

Seven-Spot:

$$p_{D(\text{pat})} = \ln\frac{d}{r_w} - 0.569. \quad \ldots\ldots (16)$$

Nine-Spot:

$$p_{D(\text{pat})} = \ln\frac{d}{r_w} - 0.272 - \frac{1}{2} \times \frac{0.693}{2 + R}. \quad \ldots\ldots (17)$$

A confirmation of $p_{D(\text{pat})}$ for the nine-spot (Eq. 17) can be shown using the limiting case in which the side well rates approach zero and $R \to \infty$. For this case, the nine-spot $p_{D(\text{pat})}$ at well spacing d should be equal to the five-spot $p_{D(\text{pat})}$ at well spacing $d\sqrt{2}$; that is,

$$\ln\frac{d}{r_w} - 0.272 - \frac{1}{2} \times \frac{0.693}{2 + R} = \ln\frac{d\sqrt{2}}{r_w} - 0.619, \quad \ldots\ldots (18)$$

which the reader can verify is true for $R \to \infty$.

Comparison of Pattern Dimensionless Pressures. Given that $p_{D(\text{pat})}$ represents the flow resistance caused by the geometry or composite flow path of a pattern, just as $\ln(r_e/r_w)$ applies to pure radial flow, and that the geometries of patterns are similar, the dimensionless pressures also should be similar. **Fig. 2** compares $p_{D(\text{pat})}$ for the various patterns at several well densities for a constant r_w. At any given well density, the $p_{D(\text{pat})}$ values are within 5%.

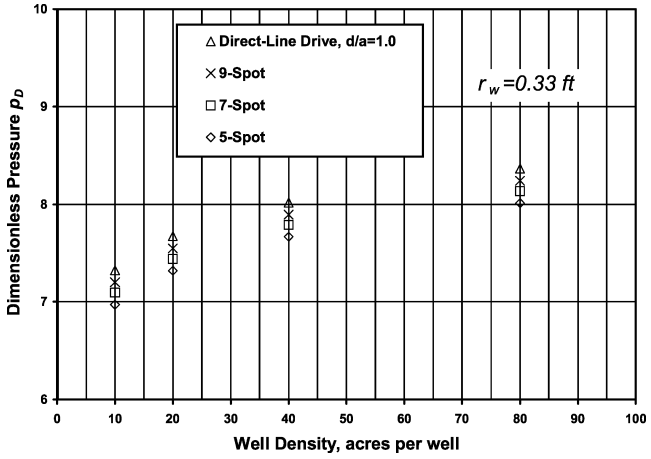

Fig. 2—Dimensionless pressures of patterns at various well densities (see Eqs. 14 through 17).

Consequently, an expression for $p_{D(\text{pat})}$ that can be used for any pattern within 2.5% is given by Eq. 19:

Any Pattern (within 2.5%):

$$p_{D(\text{pat})} = \ln\frac{d}{r_w} - 0.443. \quad \ldots\ldots\ldots\ldots\ldots\ldots\ldots\ldots (19)$$

This is an important result for patterns without a single-phase-flow equation (e.g., the skewed four-spot pattern) or for other hybrid patterns (an example of which is discussed in a later section of this paper). Eq. 19 can be used with excellent accuracy in these cases.

General Pattern Flow Equation. Based on the preceding discussion, it can be shown in a straightforward manner that a general expression for the two-phase flow rate of any pattern is given by Eq. 20:

$$\bar{q}_{\text{inj}} = \bar{\lambda}_{TI}\frac{P/I}{M_T + P/I} \times \frac{\Delta P}{p_{D(\text{pat})}} \times \frac{kh}{141.2}. \quad \ldots\ldots\ldots\ldots\ldots\ldots (20)$$

In deriving Eq. 20, it was necessary to assume that all injection well pressures and production well pressures are the same (i.e., ΔP is the same for any injector/producer pair).

Because $p_{D(\text{pat})}$ is related strictly to pattern geometry, the single-phase terms are applicable to two-phase flow, while the effects of mobility are fully accounted for with the new total mobility ratio, M_T. $p_{D(\text{pat})}$ for the nine-spot can change slightly depending on the relative corner-to-side well rates as given by R, but this dependency is small, as discussed previously.

Note also that in developing two-phase equations for the five-spot and line-drive patterns,[12] Willhite accounts for the effects of geometry using combinations of radial and linear flow segments that are coupled with mobility terms. By incorporating $\bar{p}_{\text{pat}}$, our approach has enabled the flow relationship to be generalized for all patterns by separating the effects of mobility and geometry through M_T and $p_{D(\text{pat})}$.

Normalized Flow Rates and Conductivity Ratio. Referring to Eq. 20, because the dimensionless pressures are within 5% for equivalent well spacing, comparing the individual injection well flow rates between the different patterns within a given reservoir can be based solely on the comparison of the term

$$\bar{q}_{\text{inj}} \propto \bar{\lambda}_{TI}\frac{P/I}{M_T + P/I} \quad \ldots\ldots\ldots\ldots\ldots\ldots\ldots\ldots (21)$$

because all other terms would be equal or nearly so. Eq. 21 is proportional to the individual well flow rates and does not tell us how the throughput rates of patterns would compare on a reservoir or a rate per total well basis. We can compare reservoir throughput rates as follows. Because the number of total wells associated with each injector is given by 1+*P/I,* we can define a normalized throughput rate as the rate per pattern well:

$$\tilde{q} = \frac{\bar{q}_{\text{inj}}}{1 + P/I}. \quad \ldots\ldots\ldots\ldots\ldots\ldots\ldots\ldots\ldots\ldots (22)$$

Thus, we have the full, normalized reservoir flow rate equation by combining Eq. 20 and Eq. 22:

$$\tilde{q} = \bar{\lambda}_{TI}\frac{P/I}{(M_T + P/I)(1 + P/I)} \times \frac{\Delta P}{p_{D(\text{pat})}} \times \frac{kh}{141.2}. \quad \ldots\ldots\ldots (23)$$

The total field rate, either production or injection, would then equal Eq. 23 multiplied by the total number of wells in the field. Furthermore, a reservoir conductivity ratio can be defined using Eq. 23 as follows:

$$\frac{\tilde{q}_{(1)}}{\tilde{q}_{(2)}} = \frac{(\bar{\lambda}_{TI})_1}{(\bar{\lambda}_{TI})_2}\frac{(P/I)_1}{(P/I)_2}\frac{(M_T + P/I)_2}{(M_T + P/I)_1}\frac{(1 + P/I)_2}{(1 + P/I)_1}, \quad \ldots\ldots\ldots\ldots (24)$$

where subscripts 1 and 2 refer to two different patterns and/or two points in time at a given well spacing within the same reservoir. If the flow performance of two different patterns is being compared for the time period before water breakthrough, then Eq. 24 can be reduced further by setting $(\bar{\lambda}_{TI})_1 = (\bar{\lambda}_{TI})_2$. This is because $\bar{\lambda}_{TI}$ (and, thus, M_T) will be nearly identical, varying similarly with areal sweep for any of the patterns within a given reservoir-fluid system, so that a single value for $\bar{\lambda}_{TI}$ can be assumed. The assumption of $\bar{\lambda}_{TI}$ being the same for any given pattern is especially good when M<1 and is quite acceptable when M>1. This is also shown later by the correlation between M and M_T. Thus, a more simplified form of Eq. 24 for comparisons involving the same injection fluid where $(\bar{\lambda}_{TI})_1 = (\bar{\lambda}_{TI})_2$ is given by

$$\frac{\tilde{q}_{(1)}}{\tilde{q}_{(2)}} = \frac{(P/I)_1}{(P/I)_2}\frac{(M_T + P/I)_2}{(M_T + P/I)_1}\frac{(1 + P/I)_2}{(1 + P/I)_1}. \quad \ldots\ldots\ldots\ldots\ldots (25)$$

Conductivity Relationships

Eq. 25 provides an easy method to quickly determine the relative flow performance of the various patterns before water breakthrough by comparing the *P/I*s of all the patterns [as $(P/I)_1$] relative to a base pattern [as $(P/I)_2$]. Using Eq. 25, the comparison involves only estimating the parameters $\bar{\lambda}_{TI}$ and $\bar{\lambda}_{TP}$. As mentioned earlier, $\bar{\lambda}_{TI}$ will be essentially the same among all the patterns in a given reservoir-fluid system before water breakthrough so that a single value for $\bar{\lambda}_{TI}$ (and, thus, M_T) can be used to compare all the pattern *P/I*s during this period.

Conductivity Relationship for M_T=1.0. The reservoir conductivity relationship for $M_T = 1.0$ is shown by **Fig. 3,** where the *P/I* of each pattern is compared with base pattern $(P/I)_2 = 1.0$.

Fig. 3 shows that when $M_T = 1.0$, the maximum reservoir flow rate is achieved at $P/I = 1.0$ (i.e., a five-spot or a line-drive pattern

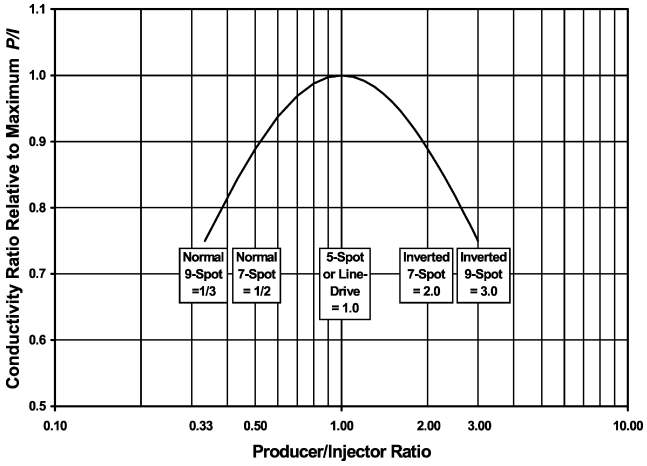

Fig. 3—Conductivity relationship for M_T=1.0.

with $d/a = 1.0$). The seven-spot and nine-spot patterns, either normal or inverted, provide 88% and 75% of the capacity of the five-spot or line-drive, respectively. In actuality, the line-drive pattern ($d/a = 1.0$) will provide 95% of the flow capacity of the five-spot because the $p_{D(\text{pat})}$ for the line drive is approximately 5% higher (see Fig. 2). Note that this conductivity relationship also could have been generated with the single-phase flow equations,[1,2] which are applicable when $M_T = 1.0$. Note also that the base P/I used in Eq. 25, $(P/I)_2$, also provides the maximum conductivity; thus, $(P/I)_2$ is denoted $(P/I)_{\max}$, as shown on the ordinate axis of Fig. 3. This convention is also used for the following comparisons of other total mobility ratios.

Conductivity Relationships for M_T=0.5 and M_T=2.0. The conductivity relationships for M_T=0.5 and M_T=2.0 are shown in **Fig. 4**. These total mobility ratios are plotted on the same graph to illustrate a few of the important relationships of Eq. 25. Note how the conductivity relationships are symmetrical around the $P/I = 1.0$ axis for these total mobility ratios, which are reciprocals of one another. The P/Is corresponding to the maximum flow capacity, $(P/I)_{\max}$, are also reciprocals; that is, when M_T=0.5, $(P/I)_{\max} = 0.7$, while for M_T=2.0, $(P/I)_{\max} = 1.428$, or 1/0.7. The producer/injector ratios providing the minimum reservoir flow capacity, or $(P/I)_{\min}$, only provide 62% of that provided by $(P/I)_{\max}$.

Even though no repeatable pattern corresponds exactly to the values of $(P/I)_{\max}$ for $M_T = 0.5$ and $M_T = 2.0$, they are sufficiently close to an actual pattern. In this case, a hybrid pattern that fills the gap between a five-spot and a seven-spot will provide the highest flow capacity. This pattern is a combination five-spot, skewed four-spot (or seven-spot in a square well arrangement), as shown in **Fig. 5.** The P/I of this pattern is either 1.67 (5:3) for an inverted pattern or 0.60 (3:5) for a normal pattern. Even though a dimensionless pressure has not been derived for this pattern, we know from Fig. 2 that $p_{D(\text{pat})}$ is largely independent of pattern configuration. Thus, for this pattern we can use $p_{D(\text{pat})}$ given by Eq. 19.

Conductivity Relationships for M_T=0.2 and M_T=5.0. Fig. 6 shows the conductivity relationships for $M_T = 0.2$ and $M_T = 5.0$. For $M_T = 0.2$, $(P/I)_{\max} = 0.45$, and for $M_T = 5.0$, $(P/I)_{\max} = 1/0.45$, or 2.22. Note from Fig. 4 and Fig. 6 that when $M_T > 1.0$, $(P/I)_{\max} > 1.0$, and when $M_T < 1.0$, $(P/I)_{\max} < 1.0$. Also, as M_T gets further away from 1.0, the difference between the conductivity at $(P/I)_{\max}$ and $(P/I)_{\min}$ gets larger. For $M_T = 0.2$ and $M_T = 5.0$, the highest and lowest conductivity patterns differ by a factor of approximately 2.

Discussion of Results. The preceding discussion shows that pattern selection can have a tremendous impact on the flow performance and, thus, on the economics of a flood. With the relative performance of the patterns now defined with respect to the total mobility ratio of the system, a rational, economically optimum pattern selection can be made using this information along with other pertinent economic variables. For example, when $M_T = 0.2$, the optimum pattern probably will not be an inverted nine-spot because this pattern would provide approximately one-half the rate that could be achieved with a normal seven-spot. Even though it provides maximum flow capacity, the normal seven-spot ultimately may not be the optimum pattern for this system, depending on the capital investment required to convert wells to injection, install the necessary fluid handling facilities, etc. Conversely, when $M_T = 5.0$, it would not be necessary to convert more injection wells than required for an inverted nine-spot because this pattern provides 98% of the maximum possible reservoir flow rate. Note that when $0.2 < M_T < 5.0$, a five-spot will provide at least 87% of the flow capacity of $(P/I)_{\max}$.

The conductivity relationship for any total mobility ratio can be determined with the procedure outlined above. The relative cost/benefit of implementing the various patterns can then be evaluated easily in reservoirs that can be considered homogeneous and isotropic, as well as in heterogeneous, isotropic reservoirs, as discussed later.

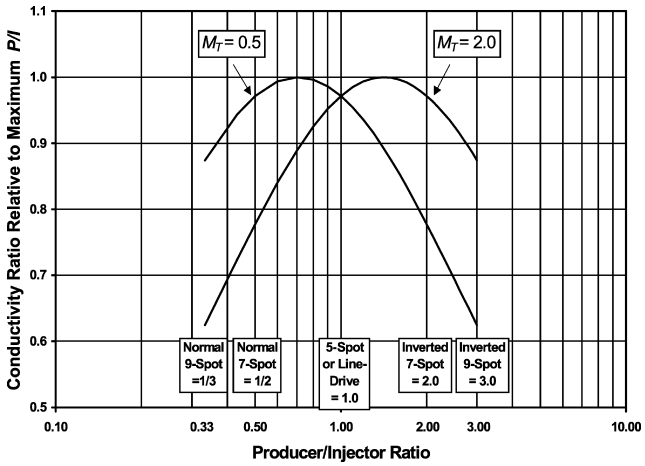

Fig. 4—Conductivity relationships for M_T=0.5 and M_T=2.0.

Pressure and Flow Relationships Including the Skin Effect

The inclusion of skin effect can be handled as an adjustment to P/I. The average reservoir pressure relationship (Eq. 1), including skin effect, is rewritten as

$$\bar{p}_{\text{pat}} = \frac{(M_T)(p_{wfI}) + (\tilde{P}/\tilde{I})(p_{wfP})}{M_T + \tilde{P}/\tilde{I}}, \quad \ldots\ldots\ldots\ldots\ldots\ldots\ldots\ldots (26)$$

where

$$\tilde{P}/\tilde{I} = P/I \, \frac{[p_{D(\text{pat})} + s_{(\text{inj})}]}{[p_{D(\text{pat})} + s_{(\text{prod})}]}, \quad \ldots\ldots\ldots\ldots\ldots\ldots\ldots\ldots (27)$$

$$s_{(\text{inj})} = \frac{\sum_{j=1}^{N_I} f_{(j)} \times s_{(j)} \times q_{(j)}}{\sum_{j=1}^{N_I} f_{(j)} \times q_{(j)}}, \quad \ldots\ldots\ldots\ldots\ldots\ldots\ldots\ldots (28)$$

and

$$s_{(\text{prod})} = \frac{\sum_{j=1}^{N_P} f_{(j)} \times s_{(j)} \times q_{(j)}}{\sum_{j=1}^{N_P} f_{(j)} \times q_{(j)}}. \quad \ldots\ldots\ldots\ldots\ldots\ldots\ldots\ldots (29)$$

$\tilde{P}/\tilde{I}$ is the effective P/I, $s_{(j)}$ is the skin factor for a given well within the pattern element, and $q_{(j)}$ is the reservoir flow rate for the same well, while all other parameters are as previously defined. Note

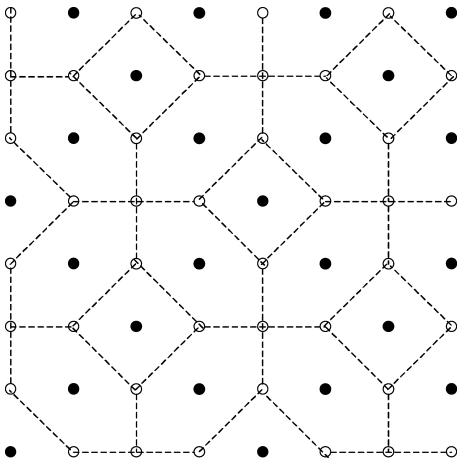

Fig. 5—Hybrid pattern with P/I=5:3 or 3:5.

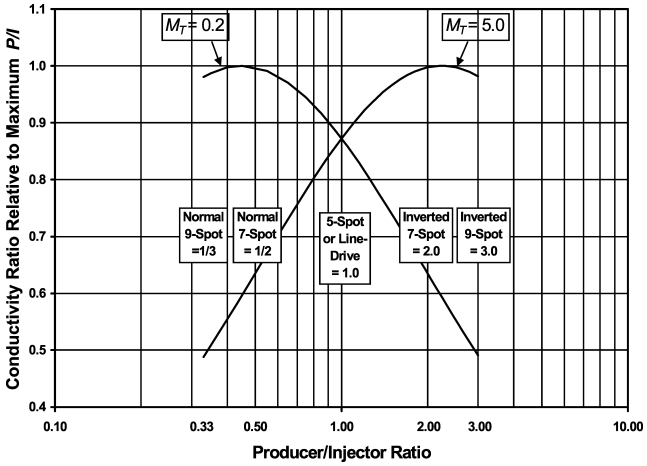

Fig. 6—Conductivity relationships for M_T=0.2 and M_T=5.0.

that $s_{(inj)}$ and $s_{(prod)}$ are the average skin factors for the injectors and producers, respectively. Even though the individual well skin factors are constant, $s_{(inj)}$ and $s_{(prod)}$ can change if the relative flow rates of the element injectors or producers change according to Eqs. 28 and 29. Changes in $s_{(inj)}$ and $s_{(prod)}$ in turn result in changes to $\tilde{P}/\tilde{I}$ (Eq. 27). The average injection well flow-rate equation (Eq. 20), including skin, becomes

$$\bar{q}_{inj} = \bar{\lambda}_{TI} \frac{\tilde{P}/\tilde{I}}{M_T + \tilde{P}/\tilde{I}} \times \frac{\Delta P}{[p_{D(pat)} + s_{(inj)}]} \times \frac{kh}{141.2}. \quad \ldots\ldots\ldots\ldots (30)$$

An interesting aspect of pattern flow behavior that can be investigated with Eqs. 26 through 30 is the incremental benefit of stimulating the producers vs. the injectors, and how in some cases little benefit is obtained by stimulating one type of well relative to the other, which depends on *P/I* and M_T. Take, for example, a system with $M_T = 0.10$ and $p_{D(pat)} = 8.2$. If the pattern is a five-spot (*P/I* = 1.0) with all wells initially having $s = 0$, then the throughput rate can be increased 50% if the injectors are stimulated to a skin of $s = -3.0$. However, only a 3.4% increase can be achieved if the same stimulation is done to the producers. There is a synergistic effect if both producers and injectors are stimulated—in this case, a 58% increase. This case is a good example of a system that is injection-capacity limited, in which an increase in production flow capacity has a relatively minor effect.

Correlation of *M* and M_T for Prebreakthrough Period

A correlation for the total mobility ratio, M_T, vs. the endpoint mobility ratio, *M,* is presented for a range of oil relative permeability curve shapes. This correlation was developed from simulation results and applies to the prebreakthrough period for a reservoir that originally is at irreducible water saturation. The correlation can be used to predict average reservoir flow rates and pressures using the equations presented. The prebreakthrough performance is treated because of its significance to the economics of a project.

Correlation Methodology. Willhite[12] shows how a range of oil relative permeability curves can be obtained based on varying the exponent *m* in the relative permeability relationship given by

$$k_{ro} = \alpha_1 (1 - S_{wD})^m, \quad \ldots\ldots\ldots\ldots (31)$$

where

$$S_{wD} = \frac{S_w - S_{iw}}{1 - S_{or} - S_{iw}}. \quad \ldots\ldots\ldots\ldots (32)$$

The water relative permeability is given by the relationship

$$k_{rw} = \alpha_2 S_{wD}{}^n. \quad \ldots\ldots\ldots\ldots (33)$$

Fig. 7 shows the oil relative permeability curves calculated with Eq. 31 for $m = 1$, 2, 3, 4, and 5 and for $\alpha_1 = 1.0$, as also presented in Ref. 12. The water relative permeability curve calculated from Eq. 33 for $n = 2.0$ is also shown, where $\alpha_2 = 0.10$. Note that only the exponents *m* and *n* (primarily *m*) are characteristic to the correlation to be presented, while the endpoint relative permeabilities are simply scaling factors; thus, any endpoint relative permeabilities can be used in the correlation. For the correlation to be presented, only the oil exponent *m* was varied, while the water exponent *n* was fixed at $n = 2.0$.

The correlation shown below is based on the average rate before water breakthrough, where M_T was back-calculated according to a rearranged form of Eq. 20,

$$M_T = \frac{P/I}{\left[\frac{kh\Delta P(P/I)\bar{\lambda}_{TP}}{141.2 p_{D(pat)} q_{avg}} - 1\right]}. \quad \ldots\ldots\ldots\ldots (34)$$

Note that $\bar{\lambda}_{TI}$ is calculated from the value of M_T obtained from the correlation and the specific endpoint value of $\bar{\lambda}_{TP}$ for a given reservoir, with $\bar{\lambda}_{TI} = M_T \bar{\lambda}_{TP}$.

Table 1 shows the correlation between M_T and *M* for the oil relative permeability exponents shown in Fig. 7 (*m*=1, 2, 3, 4, and 5 for the five-spot, the inverted nine-spot, and the normal nine-spot patterns). **Fig. 8** shows this information graphically for exponents $m = 1$, 3, and 5, while **Fig. 9** shows the relationships for exponents $m = 2$ and 4.

When comparing patterns using a single value of M_T in the conductivity-ratio relationship (Eq. 25), the value for the inverted nine-spot in Table 1 should be used because patterns with higher *P/Is* are more sensitive to any variations in M_T.[20]

Determining M_T After Water Breakthrough

The equations presented also apply after water breakthrough. However, after breakthrough the calculation of $\lambda_{T\text{eff}}$ for the producing wells is further complicated by the fact that total mobility is not uniform at a given radial distance away from a producer because of the nonradial advance, or cusping, of the flood front toward the producers. This necessitates that the total mobilities at a given radial distance from a producer are first averaged according to Eq. 7b before being incorporated into the calculation given by Eq. 7a. However, the equations presented are equally valid after breakthrough.

Heterogeneous (Isotropic) Reservoirs

If the permeability is different around individual wells, as might be determined from well tests, then the permeability thickness of each

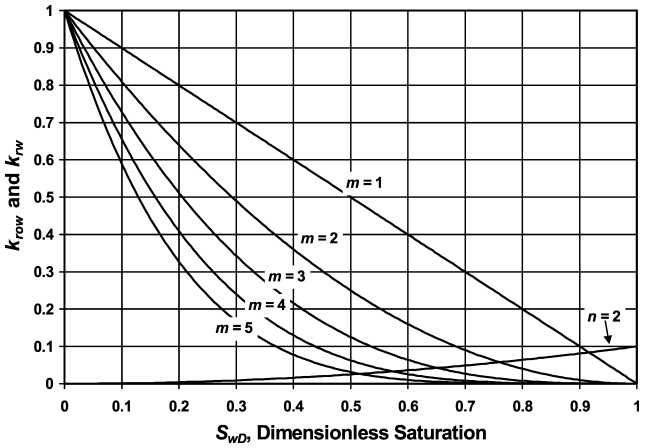

Fig. 7—Oil relative permeability curves as calculated from Eq. 31 for different *m* exponents and water relative permeability as calculated from Eq. 33 for *n*=2 (after Willhite[12]).

TABLE 1—AVERAGE M_T BEFORE WATER BREAKTHROUGH VS. M FOR VARIOUS OIL RELATIVE PERMEABILITY EXPONENTS m

M	m	5-spot	Inverted 9-spot*	Normal 9-spot
0.2	1	0.2069	0.2121	0.2110
0.2	2	0.2046	0.2103	0.2034
0.2	3	0.1843	0.1891	0.1804
0.2	4	0.1589	0.1663	0.1536
0.2	5	0.1375	0.1456	0.1330
0.5	1	0.5122	0.5186	0.5228
0.5	2	0.4809	0.4849	0.4745
0.5	3	0.4188	0.4307	0.4087
0.5	4	0.3543	0.3679	0.3396
0.5	5	0.3056	0.3144	0.2890
0.7	1	0.7114	0.7152	0.7241
0.7	2	0.6483	0.6570	0.6459
0.7	3	0.5645	0.5760	0.5449
0.7	4	0.4720	0.4864	0.4529
0.7	5	0.3993	0.4129	0.3814
1.0	1	0.9833	0.9795	0.9874
1.0	2	0.8861	0.8977	0.8763
1.0	3	0.7652	0.7758	0.7238
1.0	4	0.6453	0.6485	0.6045
1.0	5	0.5388	0.5484	0.5085
2.0	1	1.835	1.813	1.756
2.0	2	1.602	1.592	1.503
2.0	3	1.328	1.333	1.234
2.0	4	1.093	1.100	1.025
2.0	5	0.920	0.920	0.850
3.0	1	2.572	2.444	2.365
3.0	2	2.218	2.129	1.979
3.0	3	1.772	1.773	1.615
3.0	4	1.453	1.470	1.332
3.0	5	1.218	1.233	1.106
5.0	1	3.628	3.494	3.238
5.0	2	3.071	2.989	2.727
5.0	3	2.536	2.468	2.210
5.0	4	2.079	2.075	1.835
5.0	5	1.755	1.748	1.564

*When comparing patterns using Eq. 25, M_T for the inverted nine-spot can be used for all patterns because this will minimize error in the conductivity ratio. This can be tested by using Eq. 24 and substituting actual pattern values from this table; see that errors will be less than 2%.

pattern well can be incorporated into the average effective relative total mobility calculation (Eq. 3) to result in an average effective absolute total mobility for injection and production as

$$\overline{\lambda}_{TI(\text{abs})} = \frac{\sum_{j=1}^{N_I} f_{(j)} \times \lambda_{\text{Teff}(j)} \times kh_{(j)}}{\sum_{j=1}^{N_I} f_{(j)}} \quad \ldots\ldots\ldots\ldots\ldots\ldots (35a)$$

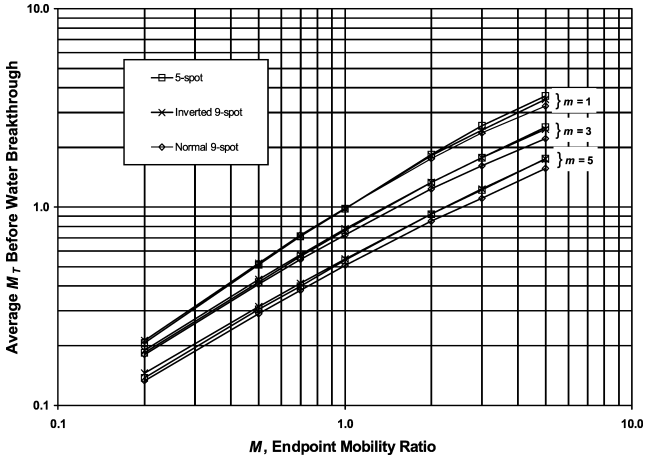

Fig. 8—Average M_T before water breakthrough vs. M for oil relative permeability exponents m=1, m=3, and m=5.

$$\text{and } \overline{\lambda}_{\text{TP(abs)}} = \frac{\sum_{j=1}^{N_P} f_{(j)} \times \lambda_{\text{Teff}(j)} \times kh_{(j)}}{\sum_{j=1}^{N_P} f_{(j)}}, \quad \ldots\ldots\ldots\ldots\ldots\ldots (35b)$$

where kh has now been included with mobility. Then, these average absolute effective total mobilities are used in the equations in the same way as those defined in Eqs. 3a and 3b. Eq. 20 then becomes

$$\overline{q}_{\text{inj}} = \overline{\lambda}_{TI(\text{abs})} \frac{P/I}{M_T + P/I} \times \frac{\Delta P}{141.2 p_{D(\text{pat})}}, \quad \ldots\ldots\ldots\ldots\ldots\ldots (36)$$

where total mobility ratio M_T is also calculated with $\overline{\lambda}_{TI(\text{abs})}$ and $\overline{\lambda}_{TP(\text{abs})}$ using Eq. 2.

Conductivity Relationships in Heterogeneous Reservoirs. If the reservoir heterogeneity is limited to variable formation permeability thickness, kh, and/or variable porosity thickness, ϕh, and not anisotropy, then the conductivity relationships presented for homogeneous systems can be used with good results if the following condition applies:

$$P/I = \frac{\sum_{j=1}^{N_P} f_{(j)} \times kh_{(j)}}{\sum_{j=1}^{N_I} f_{(j)} \times kh_{(j)}}; \quad \ldots\ldots\ldots\ldots\ldots\ldots\ldots\ldots\ldots\ldots (37)$$

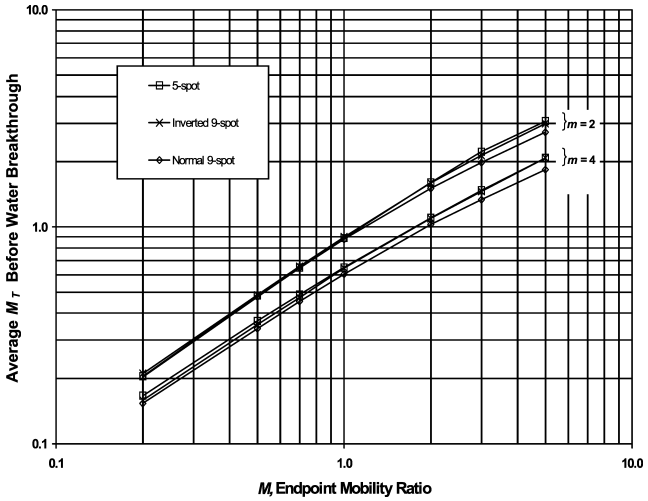

Fig. 9—Average M_T before water breakthrough vs. M for oil relative permeability exponents m=2 and m=4.

that is, the total permeability thickness of the producers to that of the injectors is approximately equal to *P/I* for any pattern that might be implemented in the reservoir. The probability of this condition applying to a given reservoir should increase as the number of wells increases.

Correlation of M vs. M_T Applied to Heterogeneous Reservoirs. The correlation of M vs. M_T presented above can be applied to heterogeneous, isotropic reservoirs if pore volume is homogeneous using the adjustments to the flow equations discussed previously. However, the correlation becomes more approximate if pore volume is heterogeneous, especially in systems in which M>1.0. This is because the pore volume around each injector determines how quickly the flood front moves away from the well (which in turn affects how the total mobility profile changes as a function of time), and the calculation of $\bar{\lambda}_{TI}$. Thus, the injection mobility profile and the resulting calculation for M_T can be somewhat different depending on the degree of pore-volume heterogeneity. This is not as big of a concern when M<1.0 because the total mobility of the injection wells, or $\bar{\lambda}_{TI}$, is established at the endpoint mobility of water more quickly than when M>1.0.

Example Calculations

The following example calculations will demonstrate the use of the equations and concepts presented in this paper, as well as the correlation for the total mobility ratio, M_T, vs. the endpoint mobility ratio, M, as presented in Table 1.

Determining Endpoint Mobility Ratio, M, and Prebreakthrough M_T. Fig. 10 shows the two-phase water/oil relative permeability curves using the correlation presented by Honarpour[22] for a water-wet sandstone reservoir with the following reservoir parameters: $S_{iw}=0.31$, $S_{or}=0.325$, $k=10.0$ md, and ϕ=0.12. Additional reservoir information is as follows: $\Delta P=4{,}190$ psi; $h=25$ ft; depth = 5,300 ft; spacing = 20 acres; $d=933.4$ ft for five-spot, nine-spot, or direct line-drive with $d/a=1.0$; $d=1.0745\times933.4=1002.9$ ft for hexagonal seven-spot; wellbore radius $r_w=0.33$ ft; $\mu_o=2.4$ cp; and $\mu_w=0.80$ cp.

Fit Relative Permeability Data. The first step is to fit the relative permeability data for the field using Eqs. 31 through 33. Fig. 10 shows how the oil relative permeability data were curve fit using an m exponent equal to 2.50 and an endpoint oil relative permeability of $\alpha_1=1.0$. As also shown in Fig. 10, it is more important to match the oil relative permeability values at higher water saturations than at lower because this region has a more significant influence on the water relative permeability in the swept portion of the reservoir. The water relative permeability data fit using Eq. 33 and an n exponent equal to 2.0 is also shown (n is fixed at 2.0 for the correlation), as is the endpoint water relative permeability, $\alpha_2=0.10$.

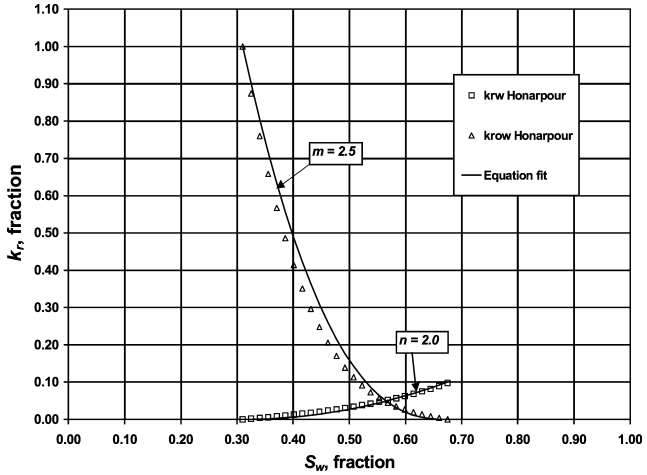

Fig. 10—Oil and water relative permeability curves using Honarpour's correlation[22] for a water-wet sandstone reservoir.

Calculate Endpoint Mobility Ratio, M. The endpoint mobility ratio M is calculated as follows:

$$M=\frac{k_{rw}/\mu_w}{k_{row}/\mu_o}=\frac{0.1/0.8}{1.0/2.4}=0.30. \quad \ldots\ldots\ldots\ldots\ldots\ldots\ldots (38)$$

Using Table 1, we see that there are no tabulated values for the mobility ratio $M=0.3$ at the exponent $m=2.5$. We can, however, interpolate a value using these parameters for the inverted nine-spot (which can be used for all patterns, as discussed earlier) and arrive at $M_T=0.291$. The conductivity relationship for $M_T=0.291$ will be very similar to that for $M_T=0.2$, shown in Fig. 6. Therefore, we expect that $(P/I)_{\max}$ is close to 0.5, or the normal seven-spot pattern, while $(P/I)_{\min}$ is 3.0, or the inverted nine-spot pattern.

Calculate Absolute Well and Reservoir Flow Rates for M_T=0.291. The absolute flow rates that will be provided by the various patterns for the reservoir system discussed earlier can be calculated using Eq. 20 as follows, with $M_T=0.291$. First, $\bar{\lambda}_{TP}$ will be equal to the endpoint total mobility of the oil, assuming that the reservoir is at S_{iw}. Thus, $\bar{\lambda}_{TP}$ is calculated as

$$\bar{\lambda}_{TP}=\frac{k_{row}}{\mu_o}=\frac{1.0}{2.4}=0.417 \text{ cp}^{-1}. \quad \ldots\ldots\ldots\ldots\ldots\ldots\ldots (39)$$

$\bar{\lambda}_{TI}$ can be calculated knowing M_T and $\bar{\lambda}_{TP}$ (Eq. 2) as

$$\bar{\lambda}_{TI}=M_T\bar{\lambda}_{TP}=0.291\times0.417=0.121 \text{ cp}^{-1}. \quad \ldots\ldots\ldots\ldots (40)$$

$p_{D(\text{pat})}$ for the inverted nine-spot can be calculated with Eq. 17, using $R=1.0$ as discussed in the text, as

$$p_{D(\text{pat})}=\ln\frac{933.4}{0.33}-0.272-\frac{1}{2}\times\frac{0.693}{2+1.0}=7.55. \quad \ldots\ldots\ldots (41)$$

The $p_{D(\text{pat})}$ can also be calculated using Eq. 19, which is within 2.5% for any pattern:

$$p_{D(\text{pat})}=\ln\frac{933.4}{0.33}-0.443=7.50. \quad \ldots\ldots\ldots\ldots\ldots\ldots (42)$$

Thus, using the parameters given above and $p_{D(\text{pat})}=7.50$, the injection well rate for the inverted nine-spot is calculated with Eq. 20 as

$$\bar{q}_{\text{inj}}=0.121\frac{3.0}{0.291+3.0}\times\frac{4190}{7.50}\times\frac{(10.0)(25)}{141.2}=109 \text{ RB/D}, \ldots (43)$$

which, according to the conditions of Table 1, is the average injection well rate before water breakthrough. The reservoir throughput rate, as given by Eq. 23, is calculated as

$$\tilde{q}=\frac{q_{\text{inj}}}{1+P/I}=\frac{109}{1+3.0}=27 \text{ RB/D/well} \quad \ldots\ldots\ldots\ldots\ldots (44)$$

(i.e., the rate per pattern well). $p_{D(\text{pat})}$ for the seven-spot is calculated according to Eq. 16. For the hexagonal seven-spot, the interwell distance must be greater than that of the nine-spot by a factor of 1.0745 for equal well density. Thus, $p_{D(\text{pat})}$ for the seven-spot is

$$p_{D(\text{pat})}=\ln\frac{(933.4)(1.0745)}{0.33}-0.569=7.45. \quad \ldots\ldots\ldots\ldots (45)$$

$p_{D(\text{pat})}$ for the seven-spot in a square well arrangement (i.e., the skewed four-spot) will be very close to that for the hexagonal seven-spot. Once again, we can use this $p_{D(\text{pat})}$ or simply use that given by Eq. 19 as 7.50. The injection well rate for the normal seven-spot ($P/I=0.5$) is likewise calculated according to Eq. 20 as

$$\bar{q}_{\text{inj}}=0.121\frac{0.5}{0.291+0.5}\times\frac{4190}{7.50}\times\frac{(10.0)(25)}{141.2}=76 \text{ RB/D}. \quad \ldots\ldots\ldots\ldots\ldots (46)$$

The reservoir throughput rate is calculated as

$$\tilde{q} = \frac{q_{inj}}{1 + P/I} = \frac{76}{1 + 0.5} = 50 \text{ RB/D/well}. \quad \ldots\ldots\ldots\ldots\ldots\ldots (47)$$

Thus, even though the individual injection well rate is lower for the normal seven-spot as compared to the inverted nine-spot, the reservoir throughput rate is 87% greater. It should be remembered that these equations are for flow rates at reservoir conditions, and formation volume factors must be included to calculate surface production and injection rates.

Influence of Skin Effect. The relative benefit of stimulating the injectors vs. producers should also be evaluated. Using Eq. 30, it can be seen that a conductivity ratio in the presence of skin effect can be defined similarly to Eq. 25 as

$$\frac{\tilde{q}_{(1)}}{\tilde{q}_{(2)}} = \frac{(\tilde{P}/\tilde{I})_1}{(\tilde{P}/\tilde{I})_2} \frac{(M_T + \tilde{P}/\tilde{I})_2}{(M_T + \tilde{P}/\tilde{I})_1} \frac{(1 + P/I)_2}{(1 + P/I)_1} \frac{[p_{D(pat)} + s_{(inj)}]_2}{[p_{D(pat)} + s_{(inj)}]_1}. \quad \ldots\ldots (48)$$

Note that Eq. 48 involves both the physical and effective producer/injector ratios, P/I and $\tilde{P}/\tilde{P}$, respectively. If we consider stimulating only the producers to a –3.0 skin, then the effective P/I (Eq. 27) for any pattern is given by

$$\tilde{P}/\tilde{I} = P/I \times \frac{(7.5 + 0)}{(7.5 - 3.0)} = P/I \times 1.67. \quad \ldots\ldots\ldots\ldots\ldots\ldots (49)$$

If it is determined from the preceding analysis that the optimum pattern is the five-spot, then $P/I = 1.0$ and $\tilde{P}/\tilde{P} = 1.67$. Then, the increase in throughput rate from stimulating only the producers (where $\bar{p}_{(2)}$ is the zero skin reference case) according to Eq. 48 is

$$\frac{\tilde{q}_{(1)}}{\tilde{q}_{(2)}} = \frac{(1.67)_1}{(1.0)_2} \frac{(0.291 + 1.0)_2}{(0.291 + 1.67)_1} \frac{(1 + 1.0)_2}{(1 + 1.0)_1} \frac{(7.5 + 0)_2}{(7.5 + 0)_1} = 1.10, \ldots (50)$$

or only a 10% increase will result. The benefit of stimulating only the injectors to the same skin of –3.0 can be determined in the same way as

$$\frac{\tilde{q}_{(1)}}{\tilde{q}_{(2)}} = \frac{(0.60)_1}{(1.0)_2} \frac{(0.291 + 1.0)_2}{(0.291 + 0.60)_1} \frac{(1 + 1.0)_2}{(1 + 1.0)_1} \frac{(7.5 + 0)_2}{(7.5 - 3.0)_1} = 1.45 \ldots (51)$$

(i.e., a 45% increase in rate). Stimulating both producers and injectors will result in

$$\frac{\tilde{q}_{(1)}}{\tilde{q}_{(2)}} = \frac{(1.0)_1}{(1.0)_2} \frac{(0.291 + 1.0)_2}{(0.291 + 1.0)_1} \frac{(1 + 1.0)_2}{(1 + 1.0)_1} \frac{(7.5 + 0)_2}{(7.5 - 3.0)_1} = 1.67 \ldots\ldots (52)$$

(i.e., a 67% increase in throughput rate). As can be seen from Eq. 27 and Eq. 48, when both types of wells have the same skin factor, the effective P/I is equal to the physical P/I, and therefore the same improvement (67%) will be obtained regardless of the pattern. However, the relative amount of improvement attributable to the injectors vs. the producers will be different depending on P/I and M_T.

Conclusions

This paper presents new equations for steady-state pattern flow performance in isotropic reservoirs. The relationships reveal how P/I and a newly defined total mobility ratio are key mechanisms controlling pattern rates and pressures.

A single, generalized pattern flow equation unifies previous works while greatly expanding the range of application to all patterns and mobility ratios. This equation makes comparing the relative flow performance of the various patterns before breakthrough possible when used in conjunction with the correlation presented between endpoint mobility ratio and total mobility ratio. The economically optimum pattern can be determined analytically using these relationships and other pertinent economic variables.

We also show how the new relationships can be modified to include skin effect and reservoir heterogeneity. The relationships including skin effect are useful to determine the relative benefit of stimulating the pattern producers vs. injectors, which can be dramatically different depending on the pattern and total mobility ratio.

Nomenclature

a = line-drive distance between wells within same row, ft
d = interwell distance, or distance between well rows for line-drive patterns, ft
f = fraction of a well's flow rate contributing to pattern element, dimensionless
h = formation thickness, ft
k = permeability, md
k_{ro} = relative permeability to oil in the presence of water, dimensionless
k_{rw} = relative permeability to water, dimensionless
m = oil relative permeability equation exponent (see Eq. 31)
M = mobility ratio based on relative permeability endpoints, dimensionless
M_t = total mobility ratio, dimensionless (after Ref. 12)
M_T = total mobility ratio (Eq. 2), dimensionless
n = water relative permeability equation exponent (see Eq. 33)
N_I = number of injectors in pattern element
N_P = number of producers in pattern element
$p_{D(pat)}$ = steady-state pattern dimensionless pressure, dimensionless
$p_{D(SS)}$ = steady-state dimensionless pressure, dimensionless
$\bar{p}_{pat}$ = volumetric average reservoir pressure of pattern, psi
p_{wfI} = sandface pressure of injection wells, psi
p_{wfP} = sandface pressure of production wells, psi
P/I = physical producer/injector ratio, dimensionless
$(P/I)_{max}$ = producer/injector ratio of maximum conductivity, dimensionless
$(P/I)_{min}$ = producer/injector ratio of minimum conductivity, dimensionless
$\tilde{P}/\tilde{I}$ = effective producer/injector ratio in the presence of skin effect, dimensionless
$\tilde{q}$ = normalized pattern reservoir, or throughput, rate, RB/D/well
q_{avg} = average flow rate before breakthrough, RB/D
$\bar{q}_{inj}$ = average rate of pattern injectors, RB/D
$\bar{q}_{prod}$ = average rate of pattern producers, RB/D
R = ratio of corner to side-well flow rates for nine-spot, dimensionless
r_w = wellbore radius, ft
r_f = flood-front radius, ft
s = well skin factor, dimensionless
$s_{(inj)}$ = average skin factor for injectors (Eq. 28), dimensionless
$s_{(prod)}$ = average skin factor for producers (Eq. 29), dimensionless
S_{iw} = irreducible water saturation, dimensionless
S_{or} = residual oil saturation, dimensionless
S_{wD} = dimensionless water saturation (Eq. 32)
α_1 = endpoint oil relative permeability in presence of water, dimensionless
α_2 = endpoint water relative permeability, dimensionless
ΔP = interwell pressure drop from injector to producer, psi
θ = included angle of well in pattern element, radians
$\bar{\lambda}_{rf}{}^{-1}$ = average reciprocal of total mobility ("apparent visocity" in Ref. 12), cp
$\lambda_r{}^{-1}$ = reciprocal of total mobility at radial distance r ("apparent viscosity" in Ref. 12), cp
λ_T = total mobility, cp^{-1}
λ_{Teff} = effective well total mobility, cp^{-1}
$\bar{\lambda}_{T(r)}$ = average λ_T at radius r, cp^{-1}

$\bar{\lambda}_{TI}$ = average effective total mobility of injection, cp^{-1}
$\bar{\lambda}_{TP(abs)}$ = average absolute effective total mobility of injection, md-ft-cp^{-1}
$\bar{\lambda}_{TP}$ = average effective total mobility of production, cp^{-1}
$\bar{\lambda}_{TP(abs)}$ = average absolute effective total mobility of production, md-ft-cp^{-1}
μ_o = oil viscosity, cp
μ_w = water viscosity, cp
ϕ = porosity, fraction

Acknowledgments

The authors wish to thank Erdal Ozkan and Robert Thompson of the Colorado School of Mines and Neil Humphreys of ExxonMobil for their helpful review and input into the content of this paper. Also, thanks to Alda Behie (Aldanumerics Ltd., Calgary), Tony Settari (U. of Calgary, Taurus Reservoir Solutions), and Duke Engineering & Services (Calgary) for use of their black-oil simulator to generate the numerical results presented in this paper.

References

1. Muskat, M.: *Flow of Homogeneous Fluids,* IHRDC, Boston, Massachusetts (1982).
2. Deppe, J.C.: "Injection Rates—The Effect of Mobility Ratio, Area Swept, and Pattern," *SPEJ* (June 1961) 81; *Trans.,* AIME, **222.**
3. Aronofsky, J.S. and Ramey, H.J. Jr.: "Mobility Ratio—Its Influence on Injection and Production Histories in Five-Spot Water Flood," *Trans.,* AIME (1956) **207,** 205.
4. Caudle, B.H. and Witte, M.D.: "Production Potential Changes During Sweep-Out in a Five-Spot System," *JPT* (December 1959) 63; *Trans.,* AIME, **216.**
5. Nobles, M.A. and Janzen, H.B.: "Application of a Resistance Network for Studying Mobility Ratio Effects," *Trans.,* AIME (1958) **213,** 356.
6. Prats, M. *et al.:* "Prediction of Injection Rate and Production History for Multifluid Five-Spot Floods," *JPT* (May 1959) 98; *Trans.,* AIME, **216.**
7. Caudle, B.H., Hickman, B.M., and Silberberg, I.H.: "Performance of the Skewed Four-Spot Injection Pattern," *JPT* (November 1968) 1315; *Trans.,* AIME, **243.**
8. Hauber, W.C.: "Prediction of Waterflood Performance for Arbitrary Well Patterns and Mobility Ratios," *JPT* (January 1964) 95; *Trans.,* AIME, **231.**
9. Cotman, N.T., Still, G.R., and Crawford, P.B.: "Laboratory Comparison of Oil Recovery in Five-Spot and Nine-Spot Waterflood Patterns," *Prod. Monthly* (December 1962) **27,** No. 12, 10.
10. Watson, R.E., Silberberg, I.H., and Caudle, B.H.: "Model Studies of the Inverted Nine-Spot Injection Pattern," *JPT* (July 1964) 801; *Trans.,* AIME, **231.**
11. Muskat, M.: "The Theory of Nine-Spot Flooding Networks," *Prod. Monthly* (March 1948) **12,** 14.
12. Willhite, G.P.: *Waterflooding,* Textbook Series, Society of Petroleum Engineers, Richardson, Texas (1986) **3.**
13. Douglas, J. Jr., Peaceman, D.W., and Rachford, H.H. Jr.: "A Method for Calculating Multi-Dimensional Immiscible Displacement," *Trans.,* AIME (1959) **216**, 297.
14. Higgins, R.V. and Leighton, A.J.: "A Computer Method of Calculating Two-Phase Flow in Any Irregularly Bounded Porous Medium," *JPT* (June 1962) 679; *Trans.,* AIME, **225.**
15. Fanchi, J.R.: *Principles of Applied Reservoir Simulation,* Butterworth-Heinemann, Boston, Massachusetts (2001).
16. LeBlanc, J.L. and Caudle, B.H.: "A Streamline Model for Secondary Recovery," *SPEJ* (March 1971) 7.
17. Martin, J.C. and Wegner, R.E.: "Numerical Solution of Multiphase, Two-Dimensional Incompressible Flow Using Stream-Tube Relationships," *SPEJ* (October 1979) 313; *Trans.,* AIME, **267.**
18. Datta-Gupta, A.: "Streamline Simulation: A Technology Update," *JPT* (December 2000) 68.
19. Craig, F.F. Jr.: *The Reservoir Engineering Aspects of Waterflooding,* Monograph Series, SPE, Richardson, Texas (1971) **3.**
20. Hansen, C.E.: *A General Pattern Flow Theory for Maximizing Waterflooding Rates,* MS thesis, Colorado School of Mines, Golden, Colorado (May 2001).
21. Dyes, A.B., Caudle, B.H., and Erickson, R.A.: "Oil Production After Breakthrough—As Influenced by Mobility Ratio," *Trans.,* AIME (1954) **201,** 81.
22. Honarpour, M., Koederitz, L., and Harvey, A.H.: *Relative Permeability of Petroleum Reservoirs,* CRC Press, LLC (1986).

Appendix A—Derivation of $p_{D(pat)}$ for the Nine-Spot

The equations for the nine-spot using "ideal" flow assumptions (see main text) were given by Deppe[2] as follows. In terms of the corner well sandface pressure, p_{wfc}, the equation is

$$q = \frac{0.003541kh(\Delta P_{i,c})}{\frac{1+R}{2+R}\left(\ln\frac{d}{r_w} - 0.272\right)\mu} \quad \text{(A-1)}$$

In terms of the side well sandface pressure, p_{wfs}, the equation is

$$q = \frac{0.007082kh(\Delta P_{i,s})}{\left[\frac{3+R}{2+R}\left(\ln\frac{d}{r_w} - 0.272\right) - \frac{0.693}{2+R}\right]\mu} \quad \text{(A-2)}$$

For the single-phase case, a more general form of Eq. 1 applies that does not require that the sandface pressures of the side and corner wells be the same, as was necessary in deriving Eq. 1 for two-phase conditions. For the single-phase case, a more general definition of p_{wfI} and p_{wfP} applies[20]:

$$p_{wfI} = \frac{\sum_{j=1}^{N_I} f_{(j)} \times p_{wf(j)}}{\sum_{j=1}^{N_I} f_{(j)}} \quad \text{(A-3)}$$

and

$$p_{wfP} = \frac{\sum_{j=1}^{N_P} f_{(j)} \times p_{wf(j)}}{\sum_{j=1}^{N_P} f_{(j)}} \quad \text{(A-4)}$$

So, referring to the element of the inverted nine-spot in Fig. 1, application of Eq. A-4 will result in the following:

$$p_{wfP} = 2/3p_{wfs} + 1/3p_{wfc}. \quad \text{(A-5)}$$

Therefore, defining an interwell pressure drop, ΔP, that is consistent with the average reservoir pressure definition (Eq. 1) is given as

$$\Delta P = p_{wfI} - (2/3p_{wfs} + 1/3p_{wfc}). \quad \text{(A-6)}$$

Note that Eq. A-6 also can be written as

$$\Delta P = 1/3(p_{wfI} - p_{wfc}) + 2/3(p_{wfI} - p_{wfs}). \quad \text{(A-7)}$$

In terms of Eqs. A-1 and A-2,

$$p_{wfI} - p_{wfc} = \frac{\frac{1+R}{2+R}\left(\ln\frac{d}{r_w} - 0.272\right)q\mu}{0.003541kh} \quad \text{(A-8)}$$

and

$$p_{wfI} - p_{wfs} = \frac{\left[\frac{3+R}{2+R}\left(\ln\frac{d}{r_w} - 0.272\right) - \frac{0.693}{2+R}\right]q\mu}{0.007082kh} \quad \text{(A-9)}$$

Therefore, Eq. A-6 can be rewritten using Eqs. A-8 and A-9 as

$$\Delta P = p_{wfI} - p_{wfP}$$
$$= 1/3 \left[\frac{\frac{1+R}{2+R}\left(\ln\frac{d}{r_w} - 0.272\right)q\mu}{0.003541kh} \right]$$
$$= 2/3 \left\{ \frac{\left[\frac{3+R}{2+R}\left(\ln\frac{d}{r_w} - 0.272\right) - \frac{0.693}{2+R}\right]q\mu}{0.007082kh} \right\}. \quad \text{.....(A-10)}$$

We now have all the information necessary to solve for $p_{D(\text{pat})}$ for the nine-spot that is consistent with the definition of the generalized flow equation given by Eq. 11. Using the inverted nine-spot case, we apply the form shown by Eq. 12, which was derived using Eq. 1 and Eq. 11a:

$$\bar{q}_{\text{inj}} = \frac{kh(p_{wfI} - p_{wfP})}{141.2p_{D(\text{pat})}\mu} \times \frac{P/I}{1+P/I} \quad \text{.....(A-11)}$$

Combining Eqs. A-10 and A-11 and substituting $P/I = 3.0$ for the inverted nine-spot, we solve for $p_{D(\text{pat})}$ as shown in Eq. 17:

$$p_{D(\text{pat})} = \ln\frac{d}{r_w} - 0.272 - \frac{1}{2} \times \frac{0.693}{2+R}. \quad \text{.....(A-12)}$$

SI Metric Conversion Factors

acre × 4.046 873	E+03 =	m^2
bbl × 1.589 873	E–01 =	m^3
cp × 1.0*	E–03 =	Pa·s
ft × 3.048*	E–01 =	m
psi × 6.894 757	E+00 =	kPa

* Conversion factor is exact.

Chris E. Hansen is a reservoir engineer at EOG Resources Inc. in Denver. e-mail: chris_hansen@eogresources.com. His current responsibilities include reservoir studies and development optimization in oil and gas fields throughout the Rocky Mountains and California. Previously, he has worked for other major and independent oil and gas companies in Texas and New Mexico. He holds BS and MS degrees in petroleum engineering from the Colorado School of Mines. **John R. Fanchi** is a professor of petroleum engineering at the Colorado School of Mines. e-mail: jfanchi@mines.edu. He has worked at three major oil companies and as a consultant. His publications include software, numerous articles, and four books, including *Principles of Applied Reservoir Simulation* and *Integrated Flow Modeling*. He holds a PhD degree in physics from the U. of Houston.

Errata

"Producer/Injector Ratio: The Key to Understanding Pattern Flow Performance and Optimizing Waterflood Design," by C.E. Hansen and J.R. Fanchi, which appeared in the October 2003 issue of *SPE Reservoir Evaluation & Engineering,* contained several misprints in the equations and text. The corrections are included here:

Page 318

Determining Effective Total Mobilities. The effective total mobility for a given well, $\lambda_{T\text{eff(j)}}$, is the single mobility value, k_r/μ, that represents the pressure-drop equivalent mobility between the wellbore and the average reservoir pressure contour. For any pattern well, this definition satisfies the relationship given by

$$[\bar{p}_{\text{pat}} - p_{wfl(j)}]\lambda_{T\text{eff(j)}} = p_{D(j)} q_{(j)} \frac{141.2}{kh}, \quad \ldots\ldots\ldots\ldots\ldots\ldots\ldots\ldots (5)$$

where $p_{D(j)}$ is the steady-state dimensionless pressure for a given well that accounts for the flow geometry between $p_{wf(j)}$ and $\bar{p}_{\text{pat}}$. $\lambda_{T\text{eff(j)}}$ can be estimated with the same approach outlined by Willhite for calculating an "average apparent viscosity", $\bar{\lambda}_{rf}^{-1}$, for a well[12]:

$$\bar{\lambda}_{rf}^{-1} = \frac{\int_{r_w}^{r_f} \lambda_r^{-1} \mathrm{d}r/r}{\ln(r_f/r_w)}. \quad \ldots\ldots\ldots\ldots\ldots\ldots\ldots\ldots\ldots\ldots\ldots\ldots (6)$$

This formula results from radial series averaging of total mobility between the well and some radial distance r_f. Radial flow around the wells is a good assumption for repeated patterns.[2,21] In this paper, the effective total mobility is similarly defined as

$$\lambda_{T\text{eff}} = \frac{\ln(r_{p\text{avg}}/r_w)}{\int_{r_w}^{r_{p\text{avg}}} \frac{\mathrm{d}r/r}{\bar{\lambda}_{T(r)}}}, \quad \ldots\ldots\ldots\ldots\ldots\ldots\ldots\ldots\ldots\ldots\ldots\ldots (7a)$$

Page 319

If we write general pattern flow equations for injectors and producers relative to the average reservoir pressure,

$$p_{wfI} - \bar{p}_{\text{pat}} = \frac{141.2\mu}{kh} p_{D(\text{inj})} \bar{q}_{\text{inj}} \quad \ldots\ldots\ldots\ldots\ldots\ldots\ldots\ldots (11a)$$

and $$\bar{p}_{\text{pat}} - p_{wfP} = \frac{141.2\mu}{kh} p_{D(\text{prod})} \bar{q}_{\text{prod}}, \quad \ldots\ldots\ldots\ldots\ldots\ldots\ldots\ldots (11b)$$

we can see that the term $\frac{141.2\mu}{kh} p_D$ must be the same for both injectors and producers in Eqs. 11a and 11b to satisfy Eq. 10 [i.e., $p_{D(\text{inj})} = p_{D(\text{prod})}$].

Page 325

Note that Eq. 48 involves both the physical and effective producer/injector ratios, P/I and $\tilde{P}/\tilde{I}$, respectively. If we consider stimulating only the producers to a –3.0 skin, then the effective P/I (Eq. 27) for any pattern is given by

$$\tilde{P}/\tilde{I} = P/I \times \frac{(7.5+0)}{(7.5-3.0)} = P/I \times 1.67. \quad \ldots\ldots\ldots\ldots\ldots\ldots\ldots (49)$$

If it is determined from the preceding analysis that the optimum pattern is the five-spot, then $P/I = 1.0$ and $\tilde{P}/\tilde{I} = 1.67$. Then, the increase in throughput rate from stimulating only the producers (where $\tilde{q}_{(2)}$ is the zero skin reference case) according to Eq. 48 is

$$\frac{\tilde{q}_{(1)}}{\tilde{q}_{(2)}} = \frac{(1.67)_1}{(1.0)_2} \frac{(0.291+1.0)_2}{(0.291+1.67)_1} \frac{(1+1.0)_2}{(1+1.0)_1} \frac{(7.5+0)_2}{(7.5+0)_1} = 1.10, \ldots (50)$$

or only a 10% increase will result.

Page 326

$\bar{\lambda}_{TI}$ = average effective total mobility of injection, cp^{-1}

$\bar{\lambda}_{TI\,(\text{abs})}$ = average absolute effective total mobility of injection, md-ft-cp^{-1}

$\bar{\lambda}_{TP}$ = average effective total mobility of production, cp^{-1}

$\bar{\lambda}_{TP(\text{abs})}$ = average absolute effective total mobility of production, md-ft-cp^{-1}

Page 327

$$\Delta P = p_{wfI} - p_{wfP}$$
$$= 1/3 \left[\frac{\frac{1+R}{2+R}\left(\ln\frac{d}{r_w} - 0.272\right) q\mu}{0.003541kh} \right]$$
$$+ 2/3 \left\{ \frac{\left[\frac{3+R}{2+R}\left(\ln\frac{d}{r_w} - 0.272\right) - \frac{0.693}{2+R}\right] q\mu}{0.007082kh} \right\}. \quad \ldots\ldots\ldots\ldots\ldots\ldots\ldots (A\text{-}10)$$